



Degradation and transformation of carbamazepine in aqueous medium under non-thermal plasma oxidation process

Manoj P Rayaroath, Olivier Aubry, Hervé Rabat, Eloi Marilleau, Yvan Gru, Dunpin Hong, Pascal Brault

► To cite this version:

Manoj P Rayaroath, Olivier Aubry, Hervé Rabat, Eloi Marilleau, Yvan Gru, et al.. Degradation and transformation of carbamazepine in aqueous medium under non-thermal plasma oxidation process. Chemosphere, 2024, 352, pp.141449. 10.1016/j.chemosphere.2024.141449 . hal-04463986

HAL Id: hal-04463986

<https://hal.science/hal-04463986>

Submitted on 17 Feb 2024

HAL is a multi-disciplinary open access archive for the deposit and dissemination of scientific research documents, whether they are published or not. The documents may come from teaching and research institutions in France or abroad, or from public or private research centers.

L'archive ouverte pluridisciplinaire **HAL**, est destinée au dépôt et à la diffusion de documents scientifiques de niveau recherche, publiés ou non, émanant des établissements d'enseignement et de recherche français ou étrangers, des laboratoires publics ou privés.



Distributed under a Creative Commons Attribution 4.0 International License



0045-6535/© 2024 The Authors. Published by Elsevier Ltd. This is an open access article under the CC BY license (<http://creativecommons.org/licenses/by/4.0/>).

inorganic anions such as chloride and carbonate ions reduced the removal efficiency by scavenging the reactive species. Accordingly, a reduction in the removal efficiency was observed in tap water. The high-resolution mass spectrometry (HRMS) results revealed that both reactive oxygen and nitrogen species take part in the reaction process which yields many intermediate products including aromatic nitro-products. This study concluded that NTP can effectively degrade CBZ in both pure and tap water, but special attention must be paid to changes in the water quality parameters (pH, conductivity, and nitrate/nitrite ions) and the fate of nitro products.

1. Introduction

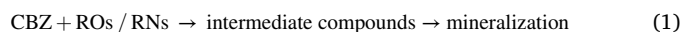
Water pollution by different kinds of organic pollutants has increased the demand for proper treatment methods all over the world. Many kinds of pollutants exist in different environmental compartments, with special interest being paid to persistent organic chemicals such as pesticides, dyes, and many halogenated chemicals, among others. A new class of chemicals that are being listed in the above category is pharmaceuticals and personal care products (PPCPs) (Wee et al., 2020; Pironti et al., 2021; Okoye et al., 2022; Zhang et al., 2022). However, exact toxicological data on these pollutants and their impact on human health, aquatic, and other environmental systems are not yet available. These kinds of chemicals are therefore called contaminants of emerging concern (CECs).

Pharmaceutically active compounds (PhACs) are the biologically active compounds used to treat diseases (Caliman and Gavrilescu, 2009; Gadipelly et al., 2014). The increase in population and hence in healthcare demands is visible from the higher number of pharmaceutical industries. As per the reports, more than 4000 drugs are prescribed and administered worldwide (aus der Beek et al., 2016). The direct disposal of waste and the disposal of unused drugs by end users lead to their undesirable presence in our environment. Another source of PhAC contamination is excreta from human or animal bodies. The pandemic in recent years further increased pharmaceutical usage (Ayati et al., 2020). This continuous usage and disposal may increase their concentration in environmental matrices, especially in water. Some kinds of pharmaceuticals detected in water bodies are antibiotics, NSAIDs, Antiepileptics, Quinolones, tetracyclines, β -blockers, etc. (Caliman and Gavrilescu, 2009; Rivera-Utrilla et al., 2013; Patel et al., 2019; Quesada et al., 2019).

An important issue associated with pharmaceuticals in environmental matrices is their biodegradation/transformation under natural environments to other metabolites, which may accumulate in the aquatic system and bioaccumulate through the food chain (Jones et al., 2005; Farré et al., 2008; Trapp et al., 2010; Rendal et al., 2011). The problem that arises due to pharmaceutical pollution is antimicrobial resistance (AMR) (Hayes et al., 2022; Miettinen and Khan, 2022). AMR is the condition where microbes such as bacteria, viruses, parasites, and fungi attain immunity towards the drugs that are usually employed to combat them (Taylor et al., 2011; Moore et al., 2020). As a result, a limited dose of the drug will not be efficient to treat human diseases. AMR pathogens have been detected in many water resources due to lack of wastewater treatment facilities in hospitals or pharmaceutical companies. This kind of infection has led to the death of millions of people all over the world (Guo et al., 2018; Muurinen et al., 2022; Thorner et al., 2022), a number that may increase in the coming years if this situation persists. A proper treatment technique is therefore required for the stringent environmental regulation of such pollutants (Oberoi et al., 2019; Papagiannaki et al., 2022).

Advanced Oxidation Processes (AOPs) are considered one of the most effective methods for the unselective treatment of wastewater containing pharmaceuticals (Rosenfeldt and Linden, 2004; Oturan and Aaron, 2014; Rayaroth et al., 2016; Miklos et al., 2018; Wang and Wang, 2020). In AOPs, highly reactive oxygen species (ROS) are generated *in situ* and react with the pollutants in a non-selective manner. However, the use of chemicals in most AOPs (techniques that use oxidants and toxic materials) may have some negative impacts on the environment.

Non-thermal plasma (NTP) oxidation is considered an emerging clean AOP technique that has the advantages of energy efficiency, performance at room temperature and atmospheric pressure, negligible use of chemicals, and ease of operation (Magureanu et al., 2015, 2021; Baloul et al., 2017; Korichi et al., 2020; Murugesan et al., 2020). NTP involves the generation of highly reactive species, ions, electrons, UV photons, etc. with the application of an electric field across the gas. The electrical discharge produces free electrons, which can react with N_2 , O_2 or H_2O to form their excited or ionized species or their dissociation; they can also excite or even ionize the dissociated species. These excited species lose energy with the emission of photons. The ionization, dissociation, and electron detachment associated with these processes result in the formation of reactive species in the discharge zone. The NTP generates a variety of reactive species such as $\bullet OH$, NO_2 , O_2^+ , etc. $\bullet OH$ is nonselective and has a strong oxidizing ability (Briset and Hnatiuc, 2012; Park et al., 2013; Lukes et al., 2014; Bradu et al., 2020), whereas NO_2 and O_2^+ are selective towards some pollutants. In addition, other neutral species such as O_3 , H_2O_2 , and other nitrogen species are also formed in the aqueous phase during this process. All these species contribute to the rapid oxidation of organic contaminants in environmental application (Eqn (1)) (Scholtz et al., 2015). Mineralization is the conversion of the initial compound to carbon dioxide, water, and inorganic ions. However, none of the oxidation processes offer direct mineralization. At the same time, the organic compound undergoes several steps such as addition, ring cleavage, bond breaking, etc. to form intermediate products. These intermediate products can be detected and analyzed at trace level by techniques such as mass spectrometry.



In the present study, the application of NTP to the removal of pharmaceutical compounds was investigated by taking carbamazepine (CBZ) as the model pollutant. CBZ is an anticonvulsant drug widely detected in various water sources (Kosjek et al., 2009; Almeida et al., 2021; Wicht et al., 2022) and has shown an AMR effect even though it is not an antibiotic (Bírošová et al., 2020). Some studies have reported the degradation of CBZ using NTP processes. Liu et al. compared the degradation efficiencies and the intermediate product formation in *ex situ* and *in situ* electric discharge on the water surface (Liu et al., 2012) and reported 100% and 91% degradation of CBZ in *ex situ* and *in situ* electric discharge respectively. Even though a color change was observed during the oxidation process (as an indication of nitro-products), no such products were identified. Singh et al. reported 99% degradation within 10 min and studied the effect of operating parameters and relevant environmental factors on the degradation of CBZ using a pulsed corona discharge (Singh et al., 2017). The proposed mechanism and the identified products were mainly correlated to the $\bullet OH$. Krause et al. used DBD treatment in a rotating drum for the degradation with special emphasis on the effect of reactor air flow rate, electrode air gap, and rotational speed. However, no data were reported on the intermediate products (Krause et al., 2011). Yu et al. made a step forward in enhancing the degradation efficiencies and combined the NTP with Fenton reagent (Fe^{2+} and H_2O_2). The combined system reported a 99% degradation in 48 min attributed to the involvement of $\bullet OH$, which was further supported by the intermediate product analysis (Yu et al., 2022). Even though all the above studies reported an evolution of significant amounts of nitrate/nitrite ions, the interference caused by them on the degradation/transformation of CBZ has not yet

been reported. Therefore, this study tried to analyse all the intermediate products formed during the NTP oxidation of CBZ using a high-resolution mass spectrometry technique. In short, this study was carried out with the following objectives: i) to study the degradation of CBZ under NTP conditions in pure water and tap water; ii) to identify the intermediate products formed during the oxidation; iii) to study the interference caused by the *in situ* generated nitrogen species on the transformation of CBZ; and iv) to study the formation and decay of the intermediate products.

2. Experimental section

2.1. Materials

The chemicals carbamazepine and formic acid were obtained from Merck Sigma Aldrich, France. HPLC-grade acetonitrile was purchased from Fisher Scientific, France. Chemical solutions were prepared with ultrapure water (referred to as pure water from here onwards) collected from a Barnstead Smart2pure (Thermo scientific) except for the tap water studies. All the chemicals used were high-purity grade and were used as received.

2.2. Degradation studies and analyses

The degradation studies were carried out in a Dielectric Barrier Discharge (DBD) plasma reactor with a multi-needle to plate configuration (Fig S1). The description of the reactor is already reported elsewhere (Baloul et al., 2017; Korichi et al., 2020). The reactor is composed of a cylindrical enclosure made of Polyvinyl Chloride (PVC) with an internal diameter of 110 mm. The high voltage electrodes are stainless steel needles (12 in number) connected to the high voltage (HV) through which the working gas is injected. They are 3 cm long and have an internal diameter of 0.4 mm and an external diameter of 0.7 mm. The plasma discharge is generated at atmospheric pressure between the tip of the needles and the surface of the liquid to be treated. The treatment of the liquid within this reactor is carried out in static mode, that is to say without liquid flow during the treatment. The distance between the HV electrodes and the liquid surface can be adjusted from 0 to 10 mm with an adjustment screw, fixed at 3.5 mm for this work. The copper ground electrode with a thickness of 0.5 mm is covered by an epoxy plate (dielectric) with a thickness of 2 mm; the assembly is set at the bottom of the enclosure and is covered by the liquid. During this work, the total flow rate of the injected gases was maintained at 100 sccm using Bronkhorst® EL-Flow flow meters. Volumes of 40 mL of carbamazepine solutions (corresponding to a liquid height of 4 mm in the reactor) were prepared in various water matrices (pure water or tap water).

The plasma was generated thanks to the smart HV pulse generator Nanogen3 from RLC Electronic®. This power supply produces a high voltage positive square pulse having a rise ramp in the range of tens of nanoseconds. The adjustable electrical parameters are the voltage (from 0 to 20 kV), the frequency (from 1 Hz to 100 kHz) and a pulse width of 1 μ s. An oscilloscope was used for the electrical measurement (LeCroy® WaveJet 354A). The dissipated power was determined from the Lissajous curve using a suitable capacitor (2 nF) placed in series in the circuit after the discharge and two HV probes (Testec® TT-HVP-2739 and Tektronix® P6015A) (Tian et al., 2021). Typical recorded HV waveforms and Lissajous curve at the selected conditions are given in Fig. 1.

The samples were drawn from the reactor using the peristaltic pump and analyzed. The concentration of pollutants during the degradation was determined using high-performance liquid chromatography (Shimadzu®; LC, 2040C 3D plus) coupled with a photodiode array detector (PDA). The detection wavelength was fixed at 283 nm. The solvent used for the separation of components from the treated CBZ was 0.1% formic acid (A) and Acetonitrile (B). A gradient elution against a C18 column (Shim-pack, 3 μ m, 150 \times 3.0 mm) obtained from Shimadzu® was performed to get a better separation of each component. Initially, the eluent was run with 5% B for 10 min, the concentration was then increased to 70% and held at the same concentration for 3 min. It was then decreased to the initial composition and allowed to stabilize for another 6 min.

The intermediates were identified by high-resolution mass spectrometry (HRMS). For HRMS acquisition data, an Ultra High Performance Liquid Chromatography (UHPLC) system (Bruker ELUTE®) coupled to a Quadrupole Time Of Flight mass spectrometer (Bruker®, Impact II Q-TOF) and interfaced by a heated electrospray ion source was used.

The LC separation was performed using an Intensity Solo C18-2 column (1.8 μ m, 100 mm \times 2.1 mm) from Bruker. The mobile phase used in ESI positive mode was 0.01 % formic acid and 5 mM ammonium formate in water (A) and 0.01 % formic acid and 5 mM ammonium formate in methanol (B). For ESI negative mode 5 mM ammonium acetate in water (A) and 5 mM ammonium acetate in methanol (B) were used. For both modes, the gradient ramp was as follows: 0–0.1 min, 96% A; 0.1–1 min to 81.7% A; 1–2.5 min to 50% A; 2.5–14 min to 0.1% A, held for 2 min, then return in 4 min to the initial conditions; and the flow ramp was: 0–1 min 0.2 ml/min; 1–2.5 min 0.223 ml/min; 2.5–14 min 0.400 ml/min; 14–19 min 0.480 ml/min; 19–20 min 0.2 ml/min. The column oven temperature and injection volume were set respectively at 40 °C and 10 μ L.

HRMS data were acquired firstly in data dependent acquisition (DDA) mode combining both full scan spectra and targeted MS/MS spectra. This first step allowed to identify and to create a data base with carbamazepine by-products. Once set up, analyses were performed in

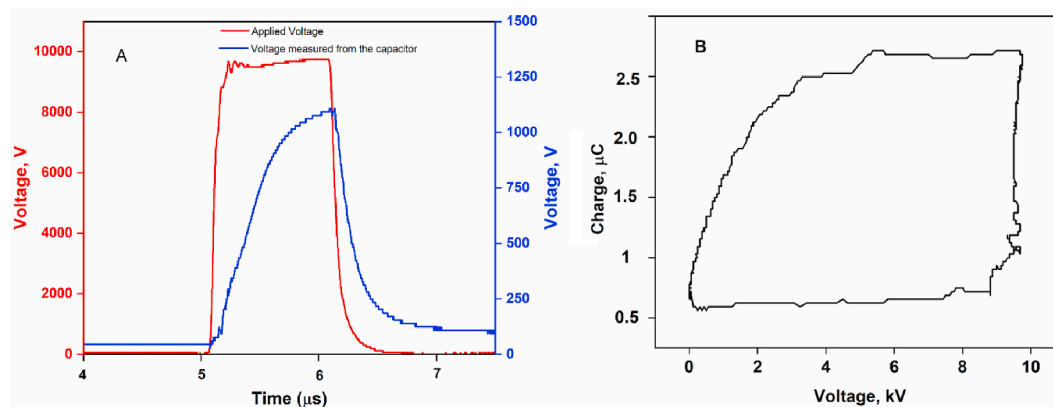


Fig. 1. HV waveforms (A) and the typical Lissajous-like curve (B) under the selected operating conditions of 10 kV, 500 Hz, and 3.5 mm needle-to-surface distance. The red line indicates the applied voltage and the blue dashed line indicates the voltage measured from the capacitor in the Lissajous method. (For interpretation of the references to color in this figure legend, the reader is referred to the Web version of this article.)

data independent analysis (DIA) combining both full scan spectra and untargeted MS/MS spectra. The resolution of the TOF spectrometer was above 60 000 at full width half maximum (FWHM) at m/z 1222. Capillary voltage was 4.5 kV in positive mode and 2.5 kV in negative mode. The probe gas temperature was set at 400 °C. The collision was performed by a flow of nitrogen at two collision energies, 24 eV and 36 eV. MS data were acquired for an m/z scan range of 30–1100 amu. The spectra rate was 3 Hz. At the beginning of each LC-HRMS run, 20 μ L of a known cluster was injected directly in the mass spectrometer with the aim to obtain an internal calibration with sub-2 ppm mass accuracy.

The time dependent evolution of some selected intermediates was monitored by an HPLC system coupled with a single quadrupole mass spectrometer (LC-MS, 2020). Single ion monitoring (SIM) was used in this case. The nitrite and nitrate ion concentrations during the NTP oxidation were measured using a MultiDirect Lovibond® photometer. An Accumet AB200 (Fisher Scientific®) system was used to measure the pH and conductivity of the solution.

The degradation percentage was calculated by Eqn (2) given below,

$$\% \text{Degradation} = \left(1 - \frac{C_t}{C_0}\right) \times 100 \quad (2)$$

where C_0 is the initial concentration and C_t is the concentration of the pollutants in g. L^{-1} after 't' hr of the treatment. The degradation kinetics was obtained by plotting $\ln(C_t/C_0)$ against time and the rate constant was calculated from the slope of the graph. The energy yield (EY in g. (kWh)^{-1}) was calculated as

$$EY = \frac{(C_0 - C_t) \times V}{\Delta t \times P} \quad (3)$$

where V is the volume of the treated solution in L, Δt is the time interval in hours, and P is the mean applied power in kW (Baloul et al., 2017).

3. Results and discussion

3.1. Degradation studies of CBZ under NTP

The degradation of CBZ under NTP conditions was performed initially. The conditions used for the plasma generation were HV 10 kV, frequency 500 Hz, and pulse duration time 1000 ns. The degradation pattern obtained is given in Fig. 2. As can be seen from the figure, 90% of the degradation was observed after 40 min of treatment with a rate constant of 0.054 min^{-1} (Fig. 2).

The EY was estimated to evaluate the treatment efficiency in terms of energy costs. It is also noted that the power during the treatment (HV-10 kV and frequency 500 Hz) was calculated in the range of 7.5–8.0 W. The EY calculated during the treatment is also given in Fig. 2. It can be seen from the figure that the EY increased from $0.19 \text{ g. (kWh)}^{-1}$ to $0.45 \text{ g. (kWh)}^{-1}$ with treatment time. A conversion rate in the range of 30–90% was observed. The EY for the degradation of 90% of the initial CBZ was compared with other oxidation methods for CBZ degradation. Liu et al. studied the degradation of CBZ by an *in situ* and *ex situ* DBD electric discharge. The EY calculated for the *ex situ* and *in situ* electric discharges were 2.88 and $0.16 \text{ g. (kWh)}^{-1}$ (Liu et al., 2012). On the other hand, NTP coupled with the Fenton process was performed at high power of 35.7 W for the degradation of CBZ and the EY calculated in this process was $0.025 \text{ g. (kWh)}^{-1}$ (Yu et al., 2022). In addition, EY in other AOPs was also considered. The EY for UV/oxidants (H_2O_2 or persulfate) was reported to be $1.78 \text{ g. (kWh)}^{-1}$ and those for hydro and sono cavitation processes 0.069 and $0.026 \text{ g. (kWh)}^{-1}$ respectively (Deng et al., 2013; Rao et al., 2016; Roy and Moholkar, 2021). This study showed that NTP offered a similar removal efficiency with comparable EY to that of other AOPs for CBZ degradation. In addition, compared to the above-mentioned processes, no chemicals were added in the solution in the present study. Hence NTP is a chemical-free and energetically favorable process for the degradation of pollutants, which is further supported by an earlier report (Palma et al., 2022).

The degradation percentage was calculated by Eqn (2) given below,

3.2. Effect of applied voltage amplitude on the degradation

The plasma generation and the subsequent production of reactive species in the reactor depend on applied voltage. In general, this parameter affects the intensity of the plasma discharge and thereby the formation of reactive species. In order to study this, the degradation of CBZ was carried out by varying the applied voltage amplitude. The needle-to-surface-distance was fixed at 3.5 mm, and the voltage was varied from 8 to 12 kV. The degradation efficiency and the corresponding EY by varying this parameter are given in Fig. 3. As can be seen from this figure, the highest degradation of 73% was observed at 12 kV, whereas 10 kV and 8 kV resulted in 70% and 54% degradation respectively after 20 min. The powers calculated were 4.3 W, 8 W, and 11 W for the applied voltages, 8 kV, 10 kV, and 12 kV respectively and the corresponding EY were 0.40 , 0.27 , and $0.20 \text{ g. (kWh)}^{-1}$ for the selected duration and the observed degradation. With an applied voltage change, the energy yield was higher at a lower applied voltage.

3.3. Identification of intermediates and the mechanism

The analysis of intermediate products in the degradation is a major challenge, particularly in the oxidation process. As can be seen from the HPLC chromatogram (Fig. 4), oxidation resulted in the generation of many intermediates, and their concentration evolved with time. The oxidation of the pollutants leads to the formation of many intermediates including those with carboxylic acids, and many inorganic ions such as nitrate and nitrite ions. The NTP itself generates nitrate and nitrite ions

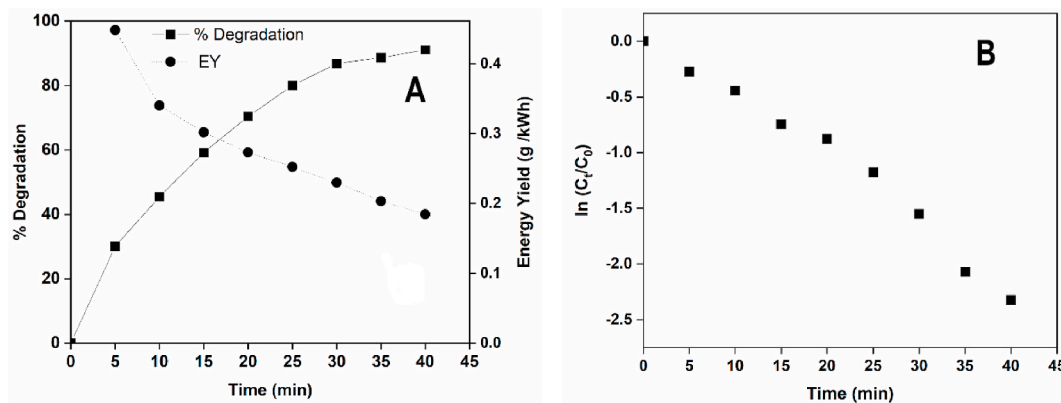


Fig. 2. (A) The degradation percentage and the corresponding EY and (B) the first order kinetics of CBZ degradation by NTP process. Experimental conditions: Needle to liquid surface distance 3.5 mm, HV – 10 kV Frequency 500 Hz, $[\text{CBZ}]_0 = 25 \text{ mg.L}^{-1}$ in pure water.

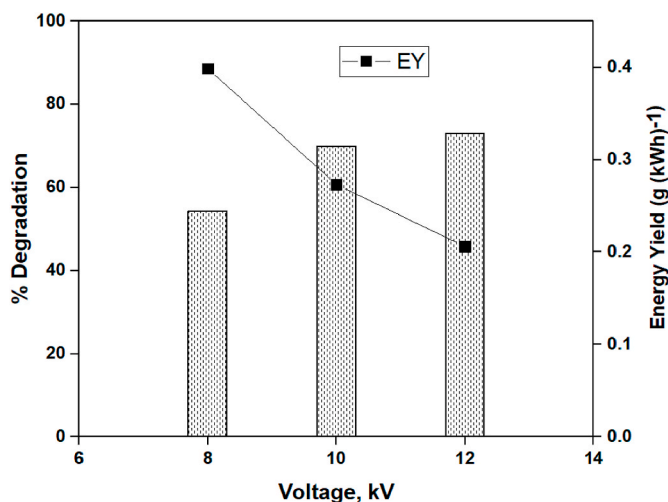


Fig. 3. Effect of applied voltage amplitude on the degradation and Energy yield with a fixed distance of 3.5 mm: Frequency 500 Hz, [CBZ]₀ = 25 mg.L⁻¹ in pure water, treatment time 20 min.

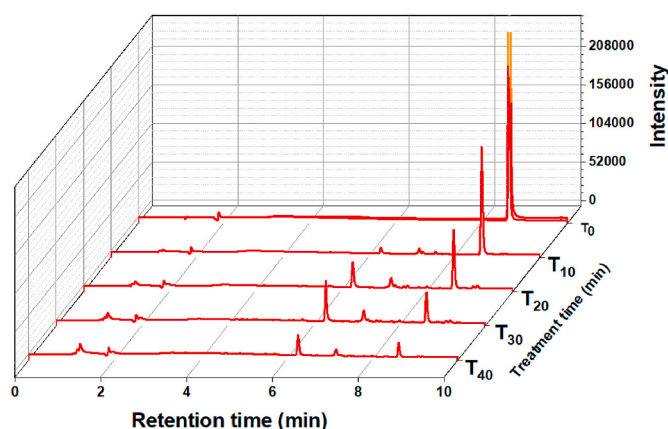


Fig. 4. Changes in the HPLC chromatogram during the NTP oxidation of CBZ. Needle to liquid surface distance 3.5 mm, HV = 10 kV Frequency 500 Hz, [CBZ]₀ = 25 mg.L⁻¹; retention time (Rt) for CBZ is 8.7 min (T₀, T₁₀, T₂₀, T₃₀, and T₄₀ indicate the treatment time).

because of the formation of soluble nitrogen oxides (Palma et al., 2021). The reactions for the formation of nitrite and nitrate ions are given in section 3.4. NTP also changes the pH and conductivity of the solution (Supporting information Fig S2). The initial pH of the CBZ solution was 6, and it decreased suddenly to 2 during oxidation. On the other hand, the conductivity of the solution increased from 0.017 mS/cm to 2.17 mS/cm after 40 min of treatment. This shows the stepwise breakdown of bonds and the subsequent release of inorganic ions that occurred during the treatment.

To determine the intermediate products, the degraded samples of CBZ were subjected to HRMS analysis, which gave the exact mass, isotopic pattern and fragmentation pattern of the intermediates. The elemental composition was defined by accurate mass of the intermediate product, measured using internal mass calibration and enhanced by the isotopic pattern fidelity represented by the "mSigma" value (Table S1). If the mSigma value is less than 50, there is less than 5 % error between the experimental and theoretical isotopic patterns. The MS/MS data for the HR-MS/MS product ions observed are listed in Table S2. Some of resulting fragments (167.0729, 180.0808, 195.0679, 210.0913) were common to several intermediates and specific to CBZ fragmentation, showed predictable losses (CONH for example). These data could be further reprocessed with different databases to give other structural

propositions (by using in silico MS/MS fragmentation). The elemental composition obtained from the HRMS also enabled the structure to be found in ChemSpider (an online database) (Hisaindee et al., 2013; Sasi et al., 2015; Rayaro et al., 2018b). The acquired MS/MS data were compared with different databanks, and thus the structures are given with a probability score and concordance with MS data.

The identified products are listed in Table 1 along with the parent CBZ molecule. For instance, the actual *m/z* value of 253 obtained from HRMS was very close to 253.0972 Da, with less than 1.6 ppm maximum error for the five isomers found, and less than 2.3% error for the experimental isotopic pattern, thus the respective elemental composition with the best score was C₁₅H₁₂N₂O₂. The *m/z* value is 16 units higher than that of CBZ. Comparison with the elemental composition of the parent CBZ (C₁₅H₁₂N₂O) shows that these intermediate products have an additional O atom. Hence the intermediate with *m/z* 253 represented the hydroxylated product, as given in Table 1. Similarly, it is likely that multiple attacks by •OH on CBZ form di- and tri-hydroxylated products. On the other hand, the elemental composition of the product with an *m/z* value of 251 was C₁₅H₁₀N₂O₂ (1 ppm error and very good experimental isotopic pattern), which is two H atoms less than the hydroxylated product. A probable structure is proposed in Table 1. In the same way, the elemental compositions of the products with *m/z* values 282 (C₁₅H₁₁N₃O₃), 296 (C₁₅H₁₃N₃O₃) and 300 (C₁₅H₁₃N₃O₄) contain an extra nitrogen atom. The attack of ROS and RNS in different positions also results in the formation of positional isomeric products. We identified five isomer products with the *m/z* values 253 and 296, three isomer products with *m/z* 241 and 282, and two isomer products with *m/z* 271 that were detected in the HRMS analysis. It is difficult to assign the exact position where the OH or NO₂ is attached to the ring. The proposed structure is therefore tentative (or one possible isomer). However, for product P2, the mSigma value was more than 50 due to observed interferences for M+1 ion (*m/z* 240) and M+2 ion (*m/z* 241), as shown in the Supporting information (Figure S3).

3.4. Degradation mechanism

The NTP process generates reactive oxygen species (ROS) such as •OH, ¹O₂, and O₂^{•-} in the medium (Gorbanev et al., 2016). Reactive nitrogen species (RNS) were also reported to be formed during the NTP process. Nitric oxides are the key species formed in the generation of RNSs. •NO is formed by the reaction of N₂ in the medium with primary oxygen species. In addition to atomic oxygen, the electron generated by the plasma process can also dissociate N₂ to form •N. The oxygen fixation reaction on NO can occur by their reaction with reactive species, resulting in the formation of nitrite radicals (•NO₂) (Brisset and Hnatiuc, 2012; Park et al., 2013; Lukes et al., 2014; Bradu et al., 2020). NOx is formed by the further oxidation of •NO₂ with reactive species and •N. All these species can also be formed in the liquid phase. Many neutral species such as HNO₂ and HNO₃ can also be formed due to the presence of humidity in the air or water molecule in the liquid phase. These species were also detected in our process (Fig. 5). The formation of RNS during the NTP process is evidenced by the NO₂ and NO₃ ions generated. Therefore, both ROS and RNS are involved in the degradation of organic pollutants.

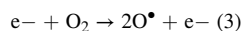
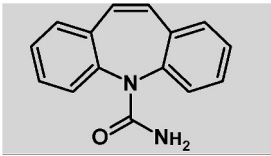
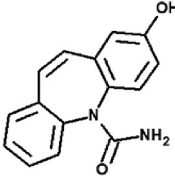
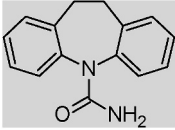
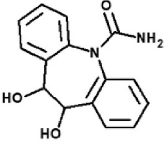
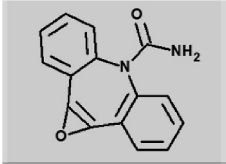
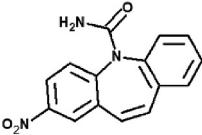
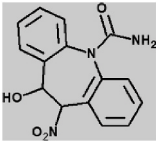
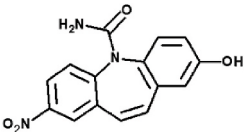


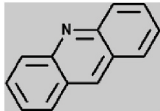
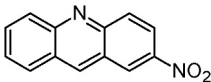
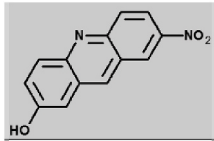
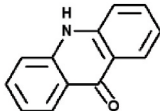
Table 1

List of products obtained using the HRMS techniques.

Product	Theoretical m/z	Molecular weight (g.mol^{-1})	Elemental composition by HRMS	Proposed Structure	ESI mode
CBZ	237.1024	236	$\text{C}_{15}\text{H}_{12}\text{N}_2\text{O}$		+
P1	253.0972	252	$\text{C}_{15}\text{H}_{12}\text{N}_2\text{O}_2$		+
P2	239.1179	238	$\text{C}_{15}\text{H}_{14}\text{N}_2\text{O}$		+
P3	271.1077	270	$\text{C}_{15}\text{H}_{14}\text{N}_2\text{O}_3$		+
P4	251.0815	250	$\text{C}_{15}\text{H}_{10}\text{N}_2\text{O}_2$		+
P5	282.0873	281	$\text{C}_{15}\text{H}_{11}\text{N}_3\text{O}_3$		+
P6	300.0979	299	$\text{C}_{15}\text{H}_{13}\text{N}_3\text{O}_4$		+
P7	296.0677	297	$\text{C}_{15}\text{H}_{11}\text{N}_3\text{O}_4$		-

(continued on next page)

Table 1 (continued)

Product	Theoretical m/z	Molecular weight (g.mol^{-1})	Elemental composition by HRMS	Proposed Structure	ESI mode
P8	180.0808	179	$\text{C}_{13}\text{H}_9\text{N}$		+
P9	225.0659	224	$\text{C}_{13}\text{H}_8\text{N}_2\text{O}_2$		+
P10	241.0608	240	$\text{C}_{13}\text{H}_8\text{N}_2\text{O}_3$		+
P11	196.0757	195	$\text{C}_{13}\text{H}_9\text{NO}$		+

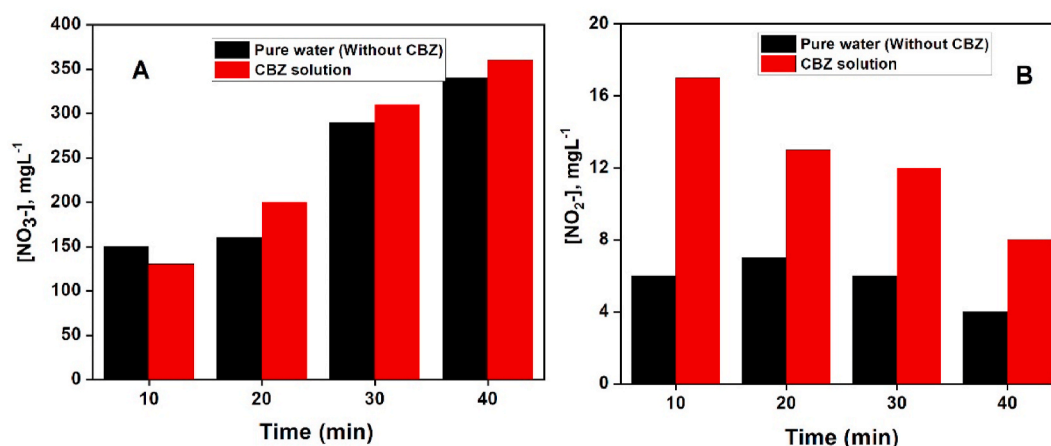
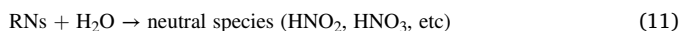
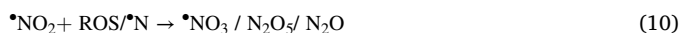


Fig. 5. Nitrate (A) and Nitrite ion (B) formation during the NTP of pure water and CBZ solution. Needle to liquid surface distance 3.5 mm, HV – 10 kV Frequency 500 Hz, $[\text{CBZ}]_0 = 25 \text{ mg.L}^{-1}$.



The attack of $\bullet\text{OH}$ on one of the C atoms in the aromatic ring of CBZ leads to the formation of hydroxy cyclohexadienyl radicals which are stabilized via resonance (Anderson et al., 1990). The hydroxyl intermediates are formed by the addition of O_2 and the elimination of HO_2^\bullet from the hydroxy cyclohexadienyl radical. For CBZ, there are three rings and many sites have access to $\bullet\text{OH}$, leading to the formation of different isomeric species of mono-hydroxylated products. A similar reaction on the hydroxylated CBZ forms tri-hydroxylated products (m/z 271, P3). The rearrangement reaction of one of the hydroxylated products leads to the formation of a product with m/z 251 (P4). The continuous attack by $\bullet\text{OH}$ results in bond breaking and further rearrangement to form products such as P8 and P10.

The RNSs especially NO_2^\bullet , caused nitration of the CBZ or its intermediate products to form nitro products. The NO_2^\bullet caused the one-electron oxidation of CBZ to form a nitrated cyclohexadienyl radical,

which can be further stabilized and finally forms the nitro products (Wei et al., 2018; Rayaroth et al., 2022). Such nitration of the parent CBZ generates a product with m/z 282 (P5). The products with m/z 300 (P6), 296 (P7), 225 (P9), and 241 (P10) are formed by the nitration reactions of either of the intermediate products of CBZ (Fig. 6).

The nitrate ion concentration increased with time in both pure water and CBZ spiked solution (Fig. 5), reaching 150 mg.L^{-1} in pure water and 130 mg.L^{-1} after 10 min of treatment, and 340 and 360 mg.L^{-1} respectively after 40 min of treatment. On the other hand, a clear difference was observed in the evolution of nitrite ions. The concentration was 6 and 17 mg.L^{-1} in the case of pure water and CBZ solution respectively after 10 min. However, it decreased to 4 and 8 after 40 min of treatment. In short, the nitrite ion concentration is high in the CBZ solution compared to pure water and decreases with time, indicating that the N in the CBZ and its intermediate products are oxidized to release nitrite ions. On the other hand, NO_3^- is not involved in the product formation. These ions either form nitrite radicals and likely undergo intercrossing reactions with the intermediate products for other nitro-products or convert to NO_3^- . This is the likely reason for the

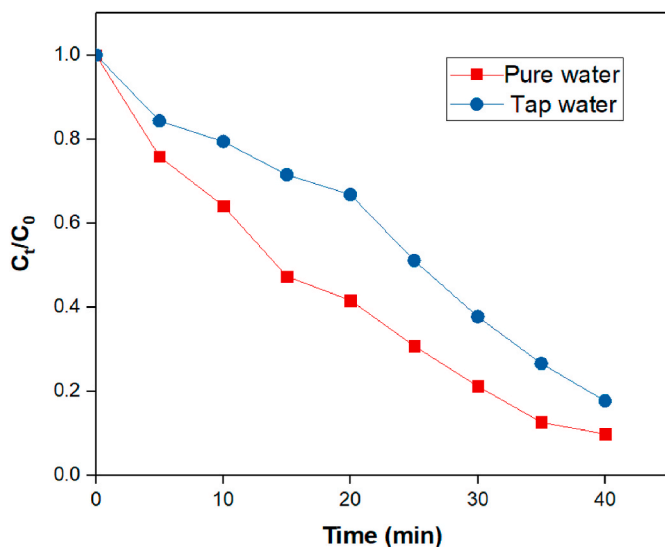


Fig. 6. The possible mechanism in the NTP process for the transformation of CBZ.

increased nitrate concentration and the decrease in nitrite ion concentration with time.

3.5. Degradation of CBZ in tap water

To gain insight into the practicability of the method, a further experiment was conducted in tap water and compared with pure water (Fig. 7). It was found that the degradation efficiency was reduced when the matrix was changed to tap water. More than 90% of degradation was observed in pure water whereas in tap water it was 83% after 40 min. The slow pH and conductivity changes indicate that CBZ degradation is slow in tap water (Fig. S4). Therefore, the decrease in the degradation is likely due to the matrix effect. The inorganic carbon concentration of the tap water was nearly 40 mg.L⁻¹, which comes mostly from carbonate ion.

Further understanding of the matrix effect was obtained from an

experiment in the presence of the most common inorganic ions. Inorganic ions, especially chloride (Cl⁻) and carbonate ions (CO₃²⁻), are the major constituents in most water matrices. They are therefore present in water contaminated with other chemicals and affect the performance of AOPs (Rayaroth et al., 2018a, 2023; Lado Ribeiro et al., 2019; Wang and Wang, 2021).

In this study, the ratio of CBZ to inorganic ion concentration was varied from 1:0 to 1:500. The degradation efficiency under varying additions of CO₃²⁻ and Cl⁻ are given in Fig. 8A and B. From these figures, it is clear that both ions reduced the degradation efficiency, with the effect of carbonate being more significant (Fig. 8A). This is due to the fact that the bimolecular rate constants for the reaction of Cl⁻ and CO₃²⁻ with •OH are $2 \times 10^7 \text{ M}^{-1}\text{s}^{-1}$ and $3.9 \times 10^8 \text{ M}^{-1}\text{s}^{-1}$, respectively, showing that CO₃²⁻ can scavenge the reactive species more than Cl⁻ (Buxton et al., 1988).

In addition, the intermediates formed in the tap water were analyzed. The products formed in both cases are the same. The products formation were monitored promptly and their intensities were plotted. A single ion monitoring (SIM) technique was used to monitor their formation at different time intervals. The main results are presented in

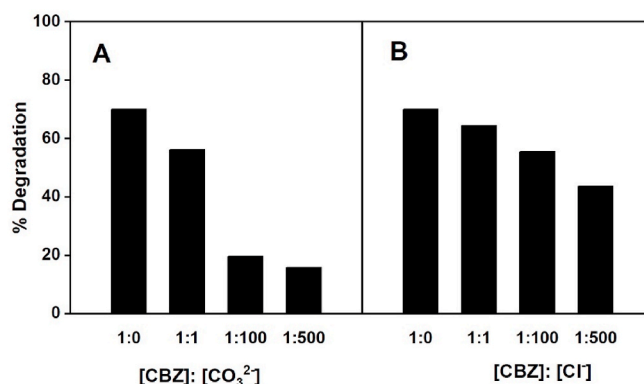


Fig. 8. Effect of CO₃²⁻ (A) and Cl⁻ (B) on the removal of CBZ; Needle to liquid surface distance 3.5 mm, HV 10 kV, Freq 500 Hz, [CBZ]₀ = 25 mg.L⁻¹, Time of treatment 20 min.

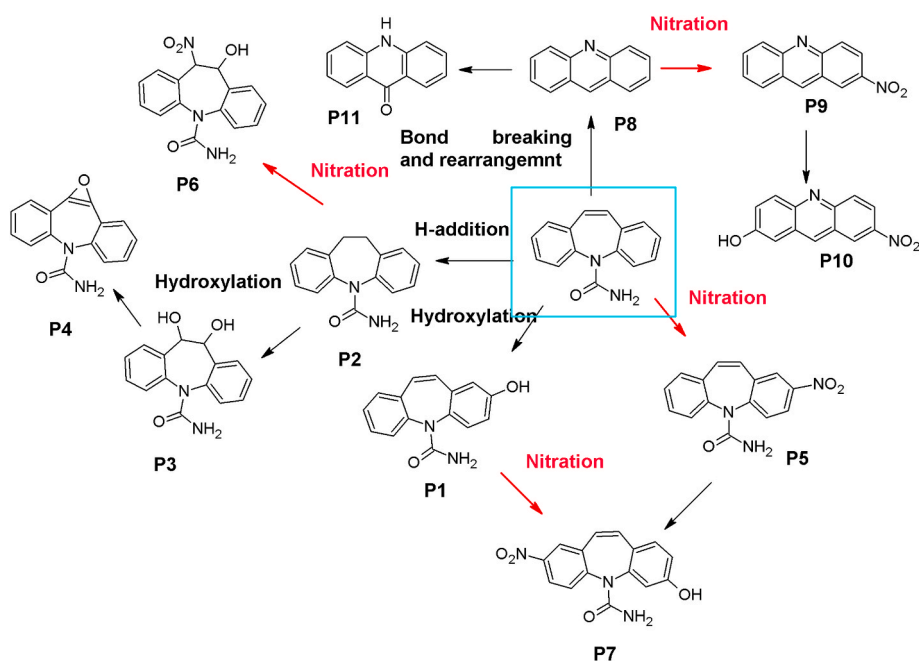


Fig. 7. Degradation of CBZ in pure and Tap water: Needle to liquid surface distance 3.5 mm, HT = 10 kV, Frequency = 500 Hz, [CBZ]₀ = 25 mg.L⁻¹.

Figs. 9 and 10. As can be seen from the figures, there are significant changes in the formation of intermediates. As an example, the intensity of the hydroxylated intermediate (m/z 253) was maximum at 25 min in pure water, but its formation was very slow in the case of tap water. A similar pattern was observed in the case of intermediates such as 251, 271, and 296. Moreover, the intensity of nitro-products such as P5, P6 and P9 is high in tap water. This is due to the fact that the RNS are less reactive towards the co-existing matrices and react more effectively with the CBZ. On the other hand, formation of the nitro-product P7 is slow in tap water. As given in the degradation pathway (Fig. 6), P7 is formed either by the hydroxylation of the nitro-product (P5) or by nitration of the hydroxylated product (P1). In this case, it is expected that the scavenging of the ROS by the co-existing matrix suppressed the hydroxylation of P5 and the RNS generated was not sufficient for nitration. With the increase in time, the concentration of RNS and P1 increases and subsequently the nitration reaction. It shows that one needs to be careful about the intermediates in the treatment of complex matrices.

4. Conclusions

This study explored the possibility of using a non-thermal plasma oxidation process in the treatment of water contaminated with the pharmaceutical compound carbamazepine (CBZ) with a special focus on the intermediate products. The degradation efficiency in both pure and real water matrices, operational parameters, and evolution of intermediate product formation was investigated in this study. Nearly complete

removal of the CBZ was attained in the NTP process with a dissipated power of 8 W. The scavenging effect by the co-existing ions (chloride and carbonate ions) reduced the removal efficiency in the real water matrix. The evolution of the reactive nitrogen species during the process was confirmed by the identification of corresponding nitro-products by high resolution mass spectrometry (HRMS) techniques. The product profiling revealed that intermediate products are formed and that their intensity initially increased and then decreased with an increase in the treatment time. However, prolonged irradiation is required to achieve the complete removal of all the intermediates. This study concluded that even though complete degradation of the CBZ is achieved within a short period, the process was not effective for the intermediate products. In addition, a reduction in pH, an increase in conductivity and the release of high concentrations of nitrite/nitrate ions into the treated water remain identified drawbacks of this process. Therefore, longer irradiation or a possible combination with nanomaterials, or other processes should be considered in real applications.

CRedit authorship contribution statement

Manoj P Rayaroth: Methodology, Investigation, Formal analysis, Writing – original draft, Writing – review & editing. **Olivier Aubry:** Conceptualization, Writing – review & editing, Supervision. **Hervé Rabat:** Methodology, Writing – review & editing. **Eloi Marilleau:** Data curation, Formal analysis, Writing – review & editing. **Yvan Gru:** Data acquisition, Writing – review & editing, Writing – review & editing.

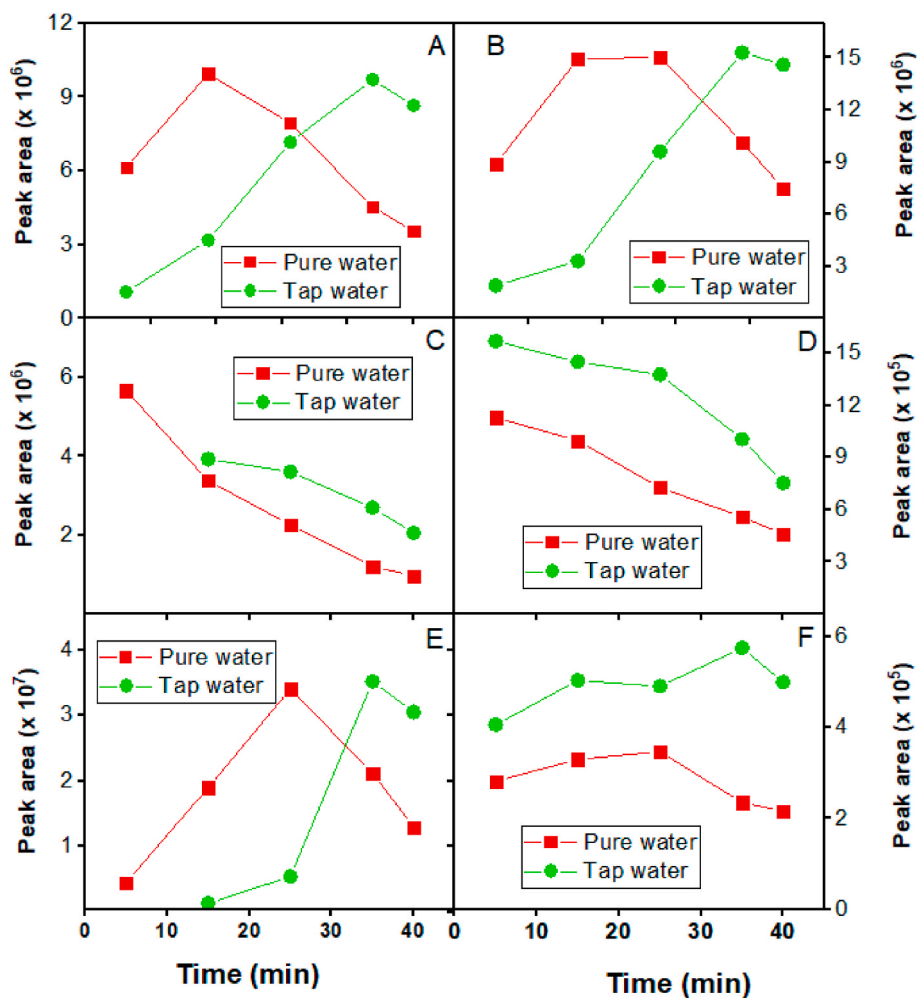


Fig. 9. Evolution of products with m/z values 271 (A, P3), 251 (B, P4), 282 (C, P5), 300 (D, P6), 180 (E, P8), 241 (F, P9); Needle to liquid surface distance 3.5 mm, HV 10 kV, Freq 500 Hz, $[CBZ]_0 = 25 \text{ mg.L}^{-1}$.

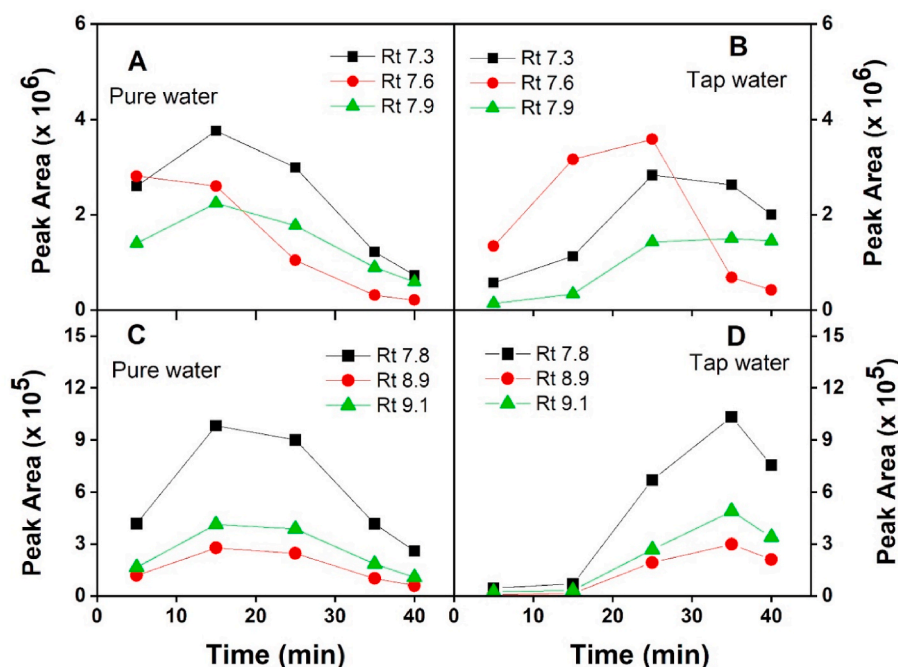


Fig. 10. Evolution of products with m/z values 253 (P1) in pure (A) and Tap water (B), and 296 (P7) in pure (C) and tap water (D) (Rt represents the retention time of the produced species); Needle to liquid surface distance 3.5 mm, HV 10 kV, Freq 500 Hz, $[CBZ]_0 = 25 \text{ mg.L}^{-1}$.

Dunpin Hong: Funding acquisition. **Pascal Brault:** Funding acquisition.

Declaration of competing interest

The authors declare that they have no known competing financial interests or personal relationships that could have appeared to influence the work reported in this paper.

Data availability

Data will be made available on request.

Acknowledgements

This work was supported by the Conseil Régional Centre-Val de Loire with grant #2021-00144786 for the project Perturb'Eau.

Appendix A. Supplementary data

Supplementary data to this article can be found online at <https://doi.org/10.1016/j.chemosphere.2024.141449>.

References

- Almeida, Á., Soares, A.M.V.M., Esteves, V.I., Freitas, R., 2021. Occurrence of the antiepileptic carbamazepine in water and bivalves from marine environments: a review. *Environ. Toxicol. Pharmacol.* 86, 103661.
- Anderson, R.F., Patel, K.B., Stratford, M.R., 1990. Absorption spectra of the hydroxycyclohexadienyl radicals of substrates for phenol hydroxylase. *J. Biol. Chem.* 265, 1952–1957.
- aus der Beek, T., Weber, F.-A., Bergmann, A., Hickmann, S., Ebert, I., Hein, A., Küster, A., 2016. Pharmaceuticals in the environment—global occurrences and perspectives. *Environ. Toxicol. Chem.* 35, 823–835.
- Ayati, N., Saiyarsarai, P., Nikfar, S., 2020. Short and long term impacts of COVID-19 on the pharmaceutical sector. *Daru* 28, 799–805.
- Baloul, Y., Aubry, O., Rabat, H., Colas, C., Maunit, B., Hong, D., 2017. Paracetamol degradation in aqueous solution by non-thermal plasma. *Eur. Phys. J. Appl. Phys.* 79.
- Bírošová, L., Lépesová, K., Grabic, R., Mackufak, T., 2020. Non-antimicrobial pharmaceuticals can affect the development of antibiotic resistance in hospital wastewater. *Environ. Sci. Pollut. Control Ser.* 27, 13501–13511.
- Bradú, C., Kutasi, K., Magureanu, M., Puač, N., Živković, S., 2020. Reactive nitrogen species in plasma-activated water: generation, chemistry and application in agriculture. *J. Phys. Appl. Phys.* 53, 223001.
- Brisset, J.-L., Hnatuc, E., 2012. Peroxynitrite: a Re-examination of the chemical properties of non-thermal discharges burning in air over aqueous solutions. *Plasma Chem. Plasma Process.* 32, 655–674.
- Buxton, G.V., Greenstock, C.L., Helman, W.P., Ross, A.B., 1988. Critical Review of rate constants for reactions of hydrated electrons, hydrogen atoms and hydroxyl radicals ($\cdot\text{OH}/\cdot\text{O}^-$ in Aqueous Solution. *J. Phys. Chem. Ref. Data* 17, 513–886.
- Caliman, F.A., Gavrilescu, M., 2009. Pharmaceuticals, personal care products and endocrine disrupting agents in the environment – a review. *CLEAN – Soil, Air, Water* 37, 277–303.
- Deng, J., Shao, Y., Gao, N., Xia, S., Tan, C., Zhou, S., Hu, X., 2013. Degradation of the antiepileptic drug carbamazepine upon different UV-based advanced oxidation processes in water. *Chem. Eng. J.* 222, 150–158.
- Farré, M.L., Pérez, S., Kantiani, L., Barceló, D., 2008. Fate and toxicity of emerging pollutants, their metabolites and transformation products in the aquatic environment. *TrAC, Trends Anal. Chem.* 27, 991–1007.
- Gadipelly, C., Pérez-González, A., Yadav, G.D., Ortiz, I., Ibáñez, R., Rathod, V.K., Marathe, K.V., 2014. Pharmaceutical industry wastewater: review of the technologies for water treatment and reuse. *Ind. Eng. Chem. Res.* 53, 11571–11592.
- Gorbanev, Y., O'Connell, D., Chechik, V., 2016. Non-thermal plasma in contact with water: the origin of species. *Chem. Eur. J.* 22, 3496–3505.
- Guo, X., Stedtfeld, R.D., Hedman, H., Eisenberg, J.N.S., Trueba, G., Yin, D., Tiedje, J.M., Zhang, L., 2018. Antibiotic resistance associated with small-scale poultry production in rural Ecuador. *Environ. Sci. Technol.* 52, 8165–8172.
- Hayes, A., May Murray, L., Catherine Stanton, I., Zhang, L., Snape, J., Hugo Gaze, W., Kaye Murray, A., 2022. Predicting selection for antimicrobial resistance in UK wastewater and aquatic environments: ciprofloxacin poses a significant risk. *Environ. Int.* 169, 107488.
- Hisaidee, S., Meetani, M.A., Rauf, M.A., 2013. Application of LC-MS to the analysis of advanced oxidation process (AOP) degradation of dye products and reaction mechanisms. *TrAC, Trends Anal. Chem.* 49, 31–44.
- Jones, O.A., Lester, J.N., Voulvoulis, N., 2005. Pharmaceuticals: a threat to drinking water? *Trends Biotechnol.* 23, 163–167.
- Korichi, N., Aubry, O., Rabat, H., Cagnon, B., Hong, D., 2020. Paracetamol degradation by catalyst enhanced non-thermal plasma process for a drastic increase in the mineralization rate. *Catalysts* 10, 959.
- Kosjek, T., Andersen, H.R., Kompere, B., Ledin, A., Heath, E., 2009. Fate of carbamazepine during water treatment. *Environ. Sci. Technol.* 43, 6256–6261.
- Krause, H., Schweiger, B., Prinz, E., Kim, J., Steinfeld, U., 2011. Degradation of persistent pharmaceuticals in aqueous solutions by a positive dielectric barrier discharge treatment. *J. Electrostat.* 69, 333–338.
- Lado Ribeiro, A.R., Moreira, N.F.F., Li Puma, G., Silva, A.M.T., 2019. Impact of water matrix on the removal of micropollutants by advanced oxidation technologies. *Chem. Eng. J.* 363, 155–173.
- Liu, Y., Mei, S., Iya-Sou, D., Cavadias, S., Ognier, S., 2012. Carbamazepine removal from water by dielectric barrier discharge: comparison of ex situ and in situ discharge on water. *Chem. Eng. Process: Process Intensif.* 56, 10–18.

- Lukes, P., Dolezalova, E., Sisrova, I., Clupek, M., 2014. Aqueous-phase chemistry and bactericidal effects from an air discharge plasma in contact with water: evidence for the formation of peroxyxynitrite through a pseudo-second-order post-discharge reaction of H₂O₂ and HNO₂. *Plasma Sources Sci. Technol.* 23, 015019.
- Magureanu, M., Bilea, F., Bradu, C., Hong, D., 2021. A review on non-thermal plasma treatment of water contaminated with antibiotics. *J. Hazard Mater.* 417, 125481.
- Magureanu, M., Mandache, N.B., Parvulescu, V.I., 2015. Degradation of pharmaceutical compounds in water by non-thermal plasma treatment. *Water Res.* 81, 124–136.
- Miettinen, M., Khan, S.A., 2022. Pharmaceutical pollution: a weakly regulated global environmental risk. *Review of European, Comparative & International Environmental Law* 31, 75–88.
- Miklos, D.B., Remy, C., Jekel, M., Linden, K.G., Drewes, J.E., Hübner, U., 2018. Evaluation of advanced oxidation processes for water and wastewater treatment – a critical review. *Water Res.* 139, 118–131.
- Moore, R.E., Millar, B.C., Moore, J.E., 2020. Antimicrobial resistance (AMR) and marine plastics: can food packaging litter act as a dispersal mechanism for AMR in oceanic environments? *Mar. Pollut. Bull.* 150, 110702.
- Murugesan, P., V, E.M., Moses, J.A., Anandharamakrishnan, C., 2020. Water decontamination using non-thermal plasma: concepts, applications, and prospects. *J. Environ. Chem. Eng.* 8, 104377.
- Muurinen, J., Muziasari, W.I., Hultman, J., Pärnänen, K., Narita, V., Lyra, C., Fadlillah, L. N., Rizki, L.P., Nurmi, W., Tiedje, J.M., Dwiprahasto, I., Hadi, P., Virta, M.P.J., 2022. Antibiotic resistomes and microbiomes in the surface water along the code river in Indonesia reflect drainage basin anthropogenic activities. *Environ. Sci. Technol.* 56, 14994–15006.
- Obero, A.S., Jia, Y., Zhang, H., Khanal, S.K., Lu, H., 2019. Insights into the fate and removal of antibiotics in engineered biological treatment systems: a critical review. *Environ. Sci. Technol.* 53, 7234–7264.
- Okoye, C.O., Okeke, E.S., Okoye, K.C., Echide, D., Andong, F.A., Chukwudozie, K.I., Okoye, H.U., Ezeonyejaku, C.D., 2022. Occurrence and fate of pharmaceuticals, personal care products (PPCPs) and pesticides in African water systems: a need for timely intervention. *Heliyon* 8, e09143.
- Oturan, M.A., Aaron, J.-J., 2014. Advanced oxidation processes in water/wastewater treatment: principles and applications. A review. *Crit. Rev. Environ. Sci. Technol.* 44, 2577–2641.
- Palma, D., Papagiannaki, D., Lai, M., Binetti, R., Sleiman, M., Minella, M., Richard, C., 2021. PFAS degradation in ultrapure and groundwater using non-thermal plasma. *Molecules* 26, 924.
- Palma, D., Richard, C., Minella, M., 2022. State of the art and perspectives about non-thermal plasma applications for the removal of PFAS in water. *Chemical Engineering Journal Advances* 10, 100253.
- Papagiannaki, D., Belay, M.H., Gonçalves, N.P.F., Robotti, E., Bianco-Prevot, A., Binetti, R., Calza, P., 2022. From monitoring to treatment, how to improve water quality: the pharmaceuticals case. *Chemical Engineering Journal Advances* 10, 100245.
- Park, D.P., Davis, K., Gilani, S., Alonzo, C.-A., Dobrynin, D., Friedman, G., Fridman, A., Rabinovich, A., Fridman, G., 2013. Reactive nitrogen species produced in water by non-equilibrium plasma increase plant growth rate and nutritional yield. *Curr. Appl. Phys.* 13, S19–S29.
- Patel, M., Kumar, R., Kishor, K., Mlsna, T., Pittman Jr., C.U., Mohan, D., 2019. Pharmaceuticals of emerging concern in aquatic systems: chemistry, occurrence, effects, and removal methods. *Chem. Rev.* 119, 3510–3673.
- Pironti, C., Ricciardi, M., Proto, A., Bianco, P.M., Montano, L., Motta, O., 2021. Endocrine-Disrupting compounds: an overview on their occurrence in the aquatic environment and human exposure. *Water* 13, 1347.
- Quesada, H.B., Baptista, A.T.A., Cusioli, L.F., Seibert, D., de Oliveira Bezerra, C., Bergamasco, R., 2019. Surface water pollution by pharmaceuticals and an alternative of removal by low-cost adsorbents: a review. *Chemosphere* 222, 766–780.
- Rao, Y., Yang, H., Xue, D., Guo, Y., Qi, F., Ma, J., 2016. Sonolytic and sonophotolytic degradation of Carbamazepine: kinetic and mechanisms. *Ultrason. Sonochem.* 32, 371–379.
- Rayaroth, M.P., Aravind, U.K., Aravindakumar, C.T., 2016. Degradation of pharmaceuticals by ultrasound-based advanced oxidation process. *Environ. Chem. Lett.* 14, 259–290.
- Rayaroth, M.P., Aravind, U.K., Aravindakumar, C.T., 2018a. Effect of inorganic ions on the ultrasound initiated degradation and product formation of triphenylmethane dyes. *Ultrason. Sonochem.* 48, 482–491.
- Rayaroth, M.P., Aravind, U.K., Aravindakumar, C.T., 2018b. Role of in-situ nitrite ion formation on the sonochemical transformation of para-aminosalicylic acid. *Ultrason. Sonochem.* 40, 213–220.
- Rayaroth, M.P., Aravindakumar, C.T., Shah, N.S., Boczkaj, G., 2022. Advanced oxidation processes (AOPs) based wastewater treatment - unexpected nitration side reactions - a serious environmental issue: a review. *Chem. Eng. J.* 430, 133002.
- Rayaroth, M.P., Boczkaj, G., Aubry, O., Aravind, U.K., Aravindakumar, C.T., 2023. Advanced oxidation processes for degradation of water pollutants—ambivalent impact of carbonate species: a review. *Water* 15, 1615.
- Rendal, C., Kusk, K.O., Trapp, S., 2011. Optimal choice of pH for toxicity and bioaccumulation studies of ionizing organic chemicals. *Environ. Toxicol. Chem.* 30, 2395–2406.
- Rivera-Utrilla, J., Sánchez-Polo, M., Ferro-García, M.Á., Prados-Joya, G., Ocampo-Pérez, R., 2013. Pharmaceuticals as emerging contaminants and their removal from water. A review. *Chemosphere* 93, 1268–1287.
- Rosenfeld, E.J., Linden, K.G., 2004. Degradation of endocrine disrupting chemicals bisphenol A, ethinyl estradiol, and estradiol during UV photolysis and advanced oxidation processes. *Environ. Sci. Technol.* 38, 5476–5483.
- Roy, K., Moholkar, V.S., 2021. Mechanistic analysis of carbamazepine degradation in hybrid advanced oxidation process of hydrodynamic cavitation/UV/persulfate in the presence of ZnO/ZnFe₂O₄. *Separ. Purif. Technol.* 270, 118764.
- Sasi, S., Rayaroth, M.P., Devadasan, D., Aravind, U.K., Aravindakumar, C.T., 2015. Influence of inorganic ions and selected emerging contaminants on the degradation of Methylparaben: a sonochemical approach. *J. Hazard Mater.* 300, 202–209.
- Scholtz, V., Pazlarova, J., Souskova, H., Khun, J., Julak, J., 2015. Nonthermal plasma — a tool for decontamination and disinfection. *Biotechnol. Adv.* 33, 1108–1119.
- Singh, R.K., Philip, L., Ramanujam, S., 2017. Rapid degradation, mineralization and detoxification of pharmaceutically active compounds in aqueous solution during pulsed corona discharge treatment. *Water Res.* 121, 20–36.
- Taylor, N.G.H., Verner-Jeffreys, D.W., Baker-Austin, C., 2011. Aquatic systems: maintaining, mixing and mobilising antimicrobial resistance? *Trends Ecol. Evol.* 26, 278–284.
- Thorner, B., Bashar, A., Ahmed, M.S., Bell, A., Trew, J., Hasan, M., Hasan, N.A., Alam, M.M., Chaput, D.L., Haque, M.M., Tyler, C.R., 2022. Antimicrobial resistance in aquaculture environments: unravelling the complexity and connectivity of the underlying societal drivers. *Environ. Sci. Technol.* 56, 14891–14903.
- Tian, T., Rabat, H., Magureanu, M., Aubry, O., Hong, D., 2021. Electrical investigation of a pin-to-plane dielectric barrier discharge in contact with water. *J. Appl. Phys.* 130, 113301.
- Trapp, S., Franco, A., Mackay, D., 2010. Activity-Based concept for transport and partitioning of ionizing organics. *Environ. Sci. Technol.* 44, 6123–6129.
- Wang, J., Wang, S., 2020. Reactive species in advanced oxidation processes: formation, identification and reaction mechanism. *Chem. Eng. J.* 401, 126158.
- Wang, J., Wang, S., 2021. Effect of inorganic anions on the performance of advanced oxidation processes for degradation of organic contaminants. *Chem. Eng. J.* 411, 128392.
- Wee, S.Y., Aris, A.Z., Yusoff, F.M., Praveena, S.M., 2020. Occurrence of multiclass endocrine disrupting compounds in a drinking water supply system and associated risks. *Sci. Rep.* 10, 17755.
- Wei, B., Sun, J., Mei, Q., An, Z., Wang, X., He, M., 2018. Theoretical study on gas-phase reactions of nitrate radicals with methoxyphenols: mechanism, kinetic and toxicity assessment. *Environ. Pollut.* 243, 1772–1780.
- Wicht, A.-J., Heye, K., Schmidt, A., Oehlmann, J., Huhn, C., 2022. The wastewater micropollutant carbamazepine in insectivorous birds—an exposure estimate. *Anal. Bioanal. Chem.* 414, 4909–4917.
- Yu, J., Yan, W., Zhu, B., Xu, Z., Hu, S., Xi, W., Lan, Y., Han, W., Cheng, C., 2022. Degradation of carbamazepine by high-voltage direct current gas–liquid plasma with the addition of H₂O₂ and Fe²⁺. *Environ. Sci. Pollut. Control Ser.* 29, 77771–77787.
- Zhang, Z., Li, X., Liu, H., Zamyadi, A., Guo, W., Wen, H., Gao, L., Nghiem, L.D., Wang, Q., 2022. Advancements in detection and removal of antibiotic resistance genes in sludge digestion: a state-of-art review. *Bioresour. Technol.* 344, 126197.